Constrained Bernstein - Jacobi hybrid polynomial curves approximation of rational Bezier curves using reparameterization

Mao Shi*

[a]*School of Mathematics and Information Science of Shaanxi Normal University, China*

Abstract

In this paper, we presented an approximation method of the rational Bézier curve by the Bernstein-Jacobi hybrid polynomial curve. A necessary and sufficient condition for $C^{(u,v)}$-continuity and sufficient condition for $G^{(u,v)}$-continuity is given. The L^1- convergence for the reparameterized rational Bézier curve is also studied. According to the orthogonality of Jacobi polynomials, calculation of the inverse of the matrix is avoided. Finally, some examples and figures were offered to demonstrate the efficiency and the simplicity of our methods.

Key words: Rational Bézier curve; Polynomial approximation; Constrained Jacobian polynomials; Hybrid curve

1. Introduction

In computer-aided geometric design (CAGD for short), geometric modeling often involves the evaluation of curve derivatives and integrals, but these two operations of rational curves are either complicated or impossible to calculate. Therefore, some experts suggest using polynomial curves to approximate rational curves to achieve intricate geometric modeling. In

*shimao@snnu.edu.cn.

1991, Sederberg and Kakimoto [1] proposed a hybrid curve for the polynomial approximation of rational curves, and its convergence conditions and boundary estimations were studied by [2, 3, 4, 5], respectively. With the progress of the research, Cai and Wang [6] applied the least-squares method to the approximation of polynomial curves of rational curves. Using dual constrained Bernstein polynomials and Chebyshev polynomials, Lewanowicz etc.[7] derived rational Bézier curves approximation by polynomial curves with endpoints constraints in the L_2-norm. Shi and Deng [8] introduced a weighted least-squares method to the field. Xu et al. [9] applied the weighted least-squares method [8] to isogeometric analysis.

Although there are a lot of research results on the polynomial approximation of rational curves, we think that the work still needs to be carried out, and that stable and efficient methods still need to be found. In a sense, reparameterization is an important optimization method to approximate rational Bézier curves. By using the reparameterization method, Sederberg [10] realized the accurate degree reduction of rational Bézier curves and points out that the degree reduction can also be given by combining with the numerical method. Later [11] [12] proposed a reparameterization-based method to approximate rational curves. The main advantage of the method in [12] is that it can preserve high-order parametric continuity or geometric continuity at the two ends of the rational curve and the approximate curve, respectively. But its necessary and sufficient condition for $C^{(u,v)}$-continuity of **Theorem 1** is incorrect since they don't consider u or v greater than the degree of rational Bézier curves. In other words, it is just a sufficient condition. On the other hand, [12] suggest that the parameter λ should not be too large for completing polynomial approximation of rational polynomial curves. This raised a question of whether the reparameterized rational Bézier curve converged, if the parameter λ is large, especially as λ tends to infinity. We will study these problems in Sections 2 and 3.

Jacobi polynomials are an important approximation tool in CAGD. Ahn [13] constructed constrained Jacobi polynomials as an error function to present a good degree reduction of Bézier curve with constraints of endpoints continuity in L^∞-norm. Chen and wang [14] defined constrained Jacobi orthogonal polynomial basis functions and used them to derive one best least-squares approximation method for multi-degree reduction of Bézier curves with constraints of endpoints continuity, and the basis transformation between Jacobi and Bernstein is used twice.

Inspired by the above-mentioned papers, we generalize [10][12][14] to the problem of a reparameterized rational Bézier curve approximation by a Bernstein -Jacobi hybrid polynomial curve.

The paper is structured as follows. Section 2 discusses some basic concepts and properties for developing our method. Section 3 states the research problems and gives the necessary and the sufficient condition of $C^{(u,v)}$-continuity and the sufficient condition of $G^{(u,v)}$-continuity for the Bernstein-Jacobi hybrid curves and the reparameterized curves. Section 4 discuss unconstrained control points of the approximation curve in the L_2 norm. Section 5 presents some numerical examples to verify the accuracy and effectiveness of the method.

2. Preliminaries

A rational Bézier curve of degree n can be defined by [15]

$$\boldsymbol{r}\left(t\right)=\frac{\sum\limits_{i=0}^{n}\omega_i\boldsymbol{r}_iB_i^n\left(t\right)}{\sum\limits_{i=0}^{n}\omega_iB_i^n\left(t\right)},\tag{1}$$

where $B_i^n(t)=\binom{n}{i}t^i(1-t)^{n-i}$, are the Bernstein basis functions of degree n, $\mathbf{r}_i$ are the control points, and ω_i are the associated positive weights.

If all weights $\omega_i = 1$, a rational Bézier curve reduces to an integer Bézier curve

$$\mathbf{p}(t) = \sum_{i=0}^{n} \mathbf{p}_i B_i^n(t). \tag{2}$$

Let $\mathbf{q}(t)$ be another Bézier curve of degree m with control points$\{\mathbf{q}_i\}_{i=0}^m$, then the product of $\mathbf{q}(t)$ and $\mathbf{p}(t)$ is given by [16]

$$\mathbf{p}(t)\mathbf{q}(t) = \sum_{k=0}^{m+n} \sum_{j=max(0,k-n)}^{min(m,k)} \frac{\binom{m}{j}\binom{n}{k-j}}{\binom{m+n}{k}} \mathbf{p}_{k-j}\mathbf{q}_j B_k^{m+n}(t). \tag{3}$$

Theorem 1. *The rth derivatives of a rational Bézier curve can be represented by the following recurrence formula*

$$\boldsymbol{r}^{(k)}(t) = \frac{\prod_{j=0}^{k-1}(2^j n) \sum_{i=0}^{2^k n} \hat{\boldsymbol{P}}_i^{[k]} B_i^{2^k n}(t)}{\sum_{i=0}^{2^k n} \omega_i^{[k]} B_i^{2^k n}(t)}, \quad k = 1, 2, ..., \tag{4}$$

where

$$\omega_i^{[0]} = \omega_i, \boldsymbol{P}_i^{[0]} = \omega_i \boldsymbol{r}_i, \hat{\boldsymbol{P}}_i^{[0]} = \boldsymbol{P}_i,$$

$$\omega_i^{[k]} = \sum_{j=\max\left(0, i-2^{k-1}n\right)}^{\min\left(i, 2^{k-1}n\right)} \frac{\binom{2^{k-1}n}{j}\binom{2^{k-1}n}{i-j}}{\binom{2^k n}{i}} \omega_j^{[k-1]} \omega_{i-j}^{[k-1]},$$

$$\boldsymbol{P}_i^{[k]} = \sum_{j=\max\left(0, i-2^{k-1}n\right)}^{\min\left(2^{k-1}n-1, i\right)} \frac{\binom{2^{k-1}n-1}{j}\binom{2^{k-1}n}{i-j}}{\binom{2^k n-1}{i}} \left(\Delta\hat{\boldsymbol{P}}_j^{[k-1]} \omega_{i-j}^{[k-1]} - \Delta\omega_j^{[k-1]} \hat{\boldsymbol{P}}_{i-j}^{[k-1]}\right),$$

and

$$\hat{\boldsymbol{P}}_i^{[k]} = \sum_{j=\max(0,i-1)}^{\min\left(2^k n-1, i\right)} \frac{\binom{2^k n-1}{j}\binom{1}{i-j}}{\binom{2^k n}{i}} \boldsymbol{P}_j^{[k]}. \tag{5}$$

Proof 1. *We use induction on k. The result is obviously valid for $k = 1$ based on* (3)*. Assumed that it is valid for some $k > 1$, then letting*

$$\hat{\boldsymbol{P}}^{[k]}(t) = \sum_{i=0}^{2^k n} \hat{\boldsymbol{P}}_i^{[k]} B_i^{2^k n}(t)$$

and

$$\omega^{[k]}(t) = \sum_{i=0}^{2^k n} \omega_i^{[k]} B_i^{2^k n}(t),$$

we have

$$\begin{aligned}
&\boldsymbol{r}^{(k+1)}(t)\\
=&\frac{\prod_{j=0}^{k-1}\left(2^j n\right)\left[\left(\hat{\boldsymbol{P}}^{[k]}(t)\right)'\omega^{[k]}(t) - \hat{\boldsymbol{P}}^{[k]}(t)\left(\omega^{[k]}(t)\right)'\right]}{\left(\omega^{[k]}(t)\right)^2}\\
=&\frac{\prod_{j=0}^{k}\left(2^j n\right)\left[\left(\sum_{i=0}^{2^k n-1}\Delta\hat{\boldsymbol{P}}_i^{[k]} B_i^{2^k n-1}(t)\right)\omega^{[k]}(t) - \hat{\boldsymbol{P}}^{[k]}(t)\left(\sum_{i=0}^{2^k n-1}\Delta\omega_i^{[k]} B_i^{2^k n-1}(t)\right)\right]}{\left(\sum_{i=0}^{2^k n}\omega_i^{[k]} B_i^{2^k n}(t)\right)^2}\\
=&\frac{\prod_{j=0}^{k}\left(2^j n\right)\left[\sum_{j=\max\left(0,i-2^k n\right)}^{\min\left(2^k n-1,i\right)}\frac{\binom{2^k n-1}{j}\binom{2^k n}{i-j}}{\binom{2^{k+1}n-1}{i}}\left(\Delta\hat{\boldsymbol{P}}_i^{[k]}\omega_{i-j}^{[k]} - \Delta\omega_i^{[k]}\hat{\boldsymbol{P}}_{i-j}^{[k]}\right)\right]}{\sum_{i=0}^{2^{k+1}n}\left(\sum_{j=\max\left(0,i-2^k n\right)}^{\min\left(i,2^k n\right)}\frac{\binom{2^k n}{j}\binom{2^k n}{i-j}}{\binom{2^{k+1}n}{i}}\omega_i^{[k]}\omega_{i-j}^{[k]}\right)B_i^{2^{k+1}n}(t)}\\
=&\frac{\prod_{j=0}^{k}\left(2^j n\right)\sum_{i=0}^{2^{k+1}n}\hat{\boldsymbol{P}}_i^{[k+1]} B_i^{2^{k+1}n}(t)}{\sum_{i=0}^{2^{k+1}n}\omega_i^{[k+1]} B_i^{2^{k+1}n}(t)}.
\end{aligned}$$

This completes the proof by induction.

If one does a Möbius parameter transformation

$$t(s) = \frac{\lambda s}{\lambda s + (1-s)},$$

the rational Bézier curve $\mathbf{r}(t)$ can be rewritten with the parameter s by

$$\boldsymbol{r}_{\lambda}\left(t\left(s\right)\right)=\frac{\sum\limits_{i=0}^{n}\lambda^{i}\omega_{i}\boldsymbol{r}_{i}B_{i}^{n}\left(s\right)}{\sum\limits_{i=0}^{n}\lambda^{i}\omega_{i}B_{i}^{n}\left(s\right)}. \tag{6}$$

Since the limit of the rational Bézier curve $\boldsymbol{r}_{\lambda}\left(t\left(s\right)\right)$ as λ approaches infinity is

$$\lim_{\lambda\to+\infty}\boldsymbol{r}_{\lambda}\left(t\left(s\right)\right)=\begin{cases}\boldsymbol{r}_{0}, & s=0,\\ \boldsymbol{r}_{n}, & s\in\left(0,1\right],\end{cases}$$

and

$$\left\|\boldsymbol{r}_{\lambda}\left(t\left(s\right)\right)\right\|\leq \underset{0\leq i\leq n}{max}\left\|\boldsymbol{r}_{i}\right\|,$$

by Bounded Convergence Theorem [17], we have the following theorem

Theorem 2. *The rational Bézier curve $\boldsymbol{r}_{\lambda}\left(t\left(s\right)\right)$ is L^{1} convergence as $\lambda\to+\infty$.*

Remark: For more details about the convergences of rational Bézier curves, the reader can refer to [18] and [19].

A Jacobi-Bernstein hybrid curve $\tilde{\mathbf{q}}(s)$ of degree m can be expressed as

$$\tilde{\mathbf{q}}(s)=\sum_{i=0}^{u}\mathbf{q}_{i}B_{i}^{m}(s)+s^{v+1}(1-s)^{u+1}\sum_{j=0}^{M}\tilde{\mathbf{q}}_{j}J_{j}^{(2u+2,2v+2)}(2s-1)+\sum_{i=m-v}^{m}\mathbf{q}_{i}B_{i}^{m}(s), \tag{7}$$

where $M=m-(u+v+2)$, $\mathbf{q}_{i}$ are the control points of the Bézier curve, $\tilde{\mathbf{q}}_{i}$ are the control points of the Jacobi curve and $J_{j}^{(2u+2,2v+2)}(2s-1)$ are the Jacobi polynomials.

It is well known that Jacobi polynomials $J_{j}^{(2u+2,2v+2)}(2s-1)$ have the following orthogonality with respect to the weight function $s^{2v+2}\left(1-s\right)^{2u+2}$

[14]

$$\chi_{i,j} = \int_0^1 s^{2v+2}(1-s)^{2u+2} J_i^{(2u+2,2v+2)}(2s-1) J_j^{(2u+2,2v+2)}(2s-1)\, ds$$
$$= \begin{cases} \frac{1}{2i+2u+2v+5} \frac{\binom{i+2u+2}{2u+2}}{\binom{i+2u+2v+4}{2u+2}} & i = j \\ 0 & i \neq j \end{cases}, \tag{8}$$

and can be represented in degree M Bernstein forms as

$$J_k^{(2u+2,2v+2)}(2s-1) = \sum_{j=0}^{M} T_{k,j} B_j^M(s), \quad k = 0, ..., M, \tag{9}$$

where

$$T_{k,j}^{(2u+2,2v+2)} = \sum_{i=\max(0,j+k-M)}^{\min(j,k)} \frac{(-1)^{k+i}\binom{k+2u+2}{i}\binom{k+2v+2}{k-i}\binom{M-k}{j-i}}{\binom{M}{j}}. \tag{10}$$

3. Problem description

In this paper, the problem of $G^{(u,v)}$ approximation of a rational Bézier curve $\mathbf{r}_\lambda(t(s))$ (6) by a polynomial curve is to find a degree m Bernstein-Jacobi hybrid polynomial curve $\tilde{\mathbf{q}}$(s) (7) such that the squared L_2-error

$$d_\lambda^2(\boldsymbol{r}, \tilde{\boldsymbol{q}}) = \int_0^1 \|\boldsymbol{r}_\lambda(t(s)) - \tilde{\boldsymbol{q}}(s)\|^2 ds \tag{11}$$

reaches the minimum under the following constrained conditions that

$$\begin{cases} \left.\frac{d^i \boldsymbol{r}_\lambda(t(s))}{ds^i}\right|_{s=0} = \left.\frac{d^i \tilde{\boldsymbol{q}}(s)}{ds^i}\right|_{s=0}, & i = 0, 1, ..., u, \\ \left.\frac{d^j \boldsymbol{r}_\lambda(t(s))}{ds^j}\right|_{s=1} = \left.\frac{d^j \tilde{\boldsymbol{q}}(s)}{ds^j}\right|_{s=1}, & j = 0, 1, ..., v. \end{cases} \tag{12}$$

By the constrained conditions (12) and the **Theorem 1**, the necessary and the sufficient condition of $C^{(u,v)}$-continuity and the sufficient condition of $G^{(u,v)}$-continuity for the Bernstein-Jacobi hybrid curve $\tilde{\mathbf{q}}(s)$ (7) and the reparameterized curve $\boldsymbol{r}_\lambda\left(t\left(s\right)\right)$ (6) is given in the following theorem.

Theorem 3. *The Bernstein-Jacobi hybrid curve* $\tilde{\mathbf{q}}(s)$ (7) *and the reparameterized curve* $\boldsymbol{r}_\lambda\left(t\left(s\right)\right)$ (6) *satisfy geometric continuity of* u, v *orders at two endpoints respectively, if and only if the following equations*

$$\mathbf{q}_k = \frac{(m-k)!}{m!}\frac{\hat{\tilde{\boldsymbol{P}}}_0^{[k]}\prod_{j=0}^{k-1}\left(2^j n\right)}{\tilde{\omega}_0^{[k]}} - \sum_{i=0}^{k-1}\left(-1\right)^{k-i}\binom{k}{i}\mathbf{q}_i,\ \ k=0,1,...,u,$$

$$\mathbf{q}_{n-l} = \frac{\left(-1\right)^l(m-l)!}{m!}\frac{\hat{\tilde{\boldsymbol{P}}}_{2^k n}^{[l]}\prod_{j=0}^{l-1}\left(2^j n\right)}{\tilde{\omega}_{2^k n}^{[l]}} - \sum_{i=1}^{l}\left(-1\right)^{i}\binom{l}{i}\mathbf{q}_{n-l+i},\ \ l=0,1,...,v,$$

are hold. where $\tilde{\omega}_i = \lambda^i\omega_i, \tilde{\boldsymbol{P}}_i = \tilde{\omega}_i\boldsymbol{r}_i,$ *and* $\hat{\boldsymbol{P}}_i^{[k]}$ *are given by* (5).

4. Unconstrained control points of the approximation curves

For simplicity, we rewrite $\tilde{\mathbf{q}}(s)$ (7) in matrix form as

$$\tilde{\mathbf{q}}\left(s\right) = \ \mathbf{B}_m^C\mathbf{Q}_m^C + \rho(s)\mathbf{J}_M\tilde{\mathbf{Q}}_M, \tag{13}$$

where $\rho(s) = s^{v+1}\left(1-s\right)^{u+1}$, $\mathbf{B}_m^C = \left(B_0^m\left(s\right), B_1^m\left(s\right), ..., B_m^m\left(s\right)\right)$, $\mathbf{Q}_m^C = \left(\boldsymbol{q}_0, ..., \boldsymbol{q}_u, 0, ..., 0, \boldsymbol{q}_{m-v}, ..., \boldsymbol{q}_m\right)^T$, $\tilde{\mathbf{Q}}_M = \left(\tilde{\boldsymbol{q}}_0, \tilde{\boldsymbol{q}}_1, ..., \tilde{\boldsymbol{q}}_M\right)^T$, and $\mathbf{J}_M = \left(J_0^{(2u+2,2v+2)}\left(2s-1\right), J_1^{(2u+2,2v+2)}\left(2s-1\right), ..., J_M^{(2u+2,2v+2)}\left(2s-1\right)\right)$.

Similarly, $\boldsymbol{r}_\lambda\left(t\left(s\right)\right)$ can also be rewritten as

$$\boldsymbol{r}_\lambda\left(t\left(s\right)\right) = \frac{\boldsymbol{B}_n\boldsymbol{\lambda}\boldsymbol{W}\boldsymbol{R}_n}{\boldsymbol{B}_n\boldsymbol{\lambda}\boldsymbol{\omega}}, \tag{14}$$

where $\boldsymbol{B}_n = \left(B_0^n\left(s\right), B_1^n\left(s\right), ..., B_n^n\left(s\right)\right)$, $\boldsymbol{\omega} = \left(\omega_0, \omega_1, ..., \omega_n\right)^T$, $\boldsymbol{R}_n = \left(\boldsymbol{r}_0, \boldsymbol{r}_1, ..., \boldsymbol{r}_{\boldsymbol{n}}\right)^T$, $\boldsymbol{\lambda} = \mathrm{diag}\left(\lambda^0, \lambda^1, ..., \lambda^n\right)$, and $\boldsymbol{W} = \mathrm{diag}\left(\omega_0, \omega_1, ..., \omega_n\right)$.

Then the alternative error function $d_\lambda^2\left(\boldsymbol{r}, \boldsymbol{q}\right)$ is expressed in matrix form as

$$d_\lambda^2(\boldsymbol{r},\boldsymbol{q}) = \int_0^1 \left\| \frac{\boldsymbol{B}_n\boldsymbol{\lambda}\boldsymbol{W}\boldsymbol{R}_n}{\boldsymbol{B}_n\boldsymbol{\lambda}\boldsymbol{\omega}} - \mathbf{B}_m^C\mathbf{Q}_m^C - \rho(s)\mathbf{J}_M\tilde{\mathbf{Q}}_M \right\|^2 ds$$

To minimize the objective function $d_\lambda^2(\boldsymbol{r},\boldsymbol{q})$, the derivatives of $d_\lambda^2(\boldsymbol{r},\boldsymbol{q})$ with respect to the elements of $\tilde{\mathbf{Q}}_M$ should be zero. That is

$$\begin{aligned}\frac{\partial d_\lambda^2(\boldsymbol{r},\boldsymbol{q})}{\partial\tilde{\mathbf{Q}}_M} &= 2\int_0^1 \rho(s)\left(\mathbf{J}_M\right)^T\left(\frac{\boldsymbol{B}_n\boldsymbol{\lambda}\boldsymbol{W}\boldsymbol{R}_n}{\boldsymbol{B}_n\boldsymbol{\lambda}\boldsymbol{\omega}} - \mathbf{B}_m^C\mathbf{Q}_m^C - \rho(s)\mathbf{J}_M\tilde{\mathbf{Q}}_M\right) ds \\ &= \mathbf{0}.\end{aligned}$$

Substituting (9) and (10) in to the above-mentioned equation, the unknown control points of the approximation curve are obtained as following

$$\begin{aligned}\tilde{\mathbf{Q}}_M &= (\boldsymbol{\chi})^{-1}\left(\int_0^1 \frac{\rho(s)\left(\mathbf{J}_M\right)^T\boldsymbol{B}_n}{\boldsymbol{B}_n\boldsymbol{\lambda}\boldsymbol{\omega}} ds\boldsymbol{\lambda}\boldsymbol{W}\boldsymbol{R}_n - \int_0^1 \rho(s)\left(\mathbf{J}_M\right)^T\mathbf{B}_m^C ds\mathbf{Q}_m^C\right), \\ &= (\boldsymbol{\chi})^{-1}\boldsymbol{T}\left(\int_0^1 \frac{\rho(s)\left(\boldsymbol{B}_M\right)^T\boldsymbol{B}_n}{\boldsymbol{B}_n\boldsymbol{\lambda}\boldsymbol{\omega}} ds\boldsymbol{\lambda}\boldsymbol{W}\boldsymbol{R}_n - \int_0^1 \rho(s)\left(\boldsymbol{B}_M\right)^T\mathbf{B}_m^C ds\mathbf{Q}_m^C\right) \\ &= (\boldsymbol{\chi})^{-1}\boldsymbol{T}\left(\boldsymbol{N}\boldsymbol{\lambda}\boldsymbol{W}\boldsymbol{R}_n - \boldsymbol{X}\mathbf{Q}_m^C\right),\end{aligned} \tag{15}$$

where $\boldsymbol{\chi} = \left(\chi_{ij}\right)_{M\times M}$, $\boldsymbol{T} = \left(T_{k,j}^{(2u+2,2v+2)}\right)_{M\times M}$,
$\boldsymbol{X} = \frac{1}{u+v+M+m+3}\frac{\binom{M}{i}\binom{m}{j}}{\binom{u+v+M+m+2}{u+1+i+j}}$ and $\boldsymbol{N} = \int_0^1 \frac{\rho(s)\left(\boldsymbol{B}_M\right)^T\boldsymbol{B}_n}{\boldsymbol{B}_n\boldsymbol{\lambda}\boldsymbol{\omega}} ds$.

In order to find an optimal value of λ such that the distance function $d_\lambda^2(\boldsymbol{r},\boldsymbol{q})$ reaches its minimum value, we inserting the control points (15) into $d_\lambda^2(\boldsymbol{r},\boldsymbol{q})$, and which can be revised as

$$\begin{aligned}d_\lambda^2(\boldsymbol{r},\boldsymbol{q}) &= \int_0^1 \left\| \frac{\boldsymbol{B}_n\boldsymbol{\lambda}\boldsymbol{W}\boldsymbol{R}_n}{\boldsymbol{B}_n\boldsymbol{\lambda}\boldsymbol{\omega}} - \mathbf{B}_m^C\mathbf{Q}_m^C - \rho(s)\mathbf{J}_M\tilde{\mathbf{Q}}_M \right\|^2 ds \\ &= \boldsymbol{R}_n^T\boldsymbol{W}\boldsymbol{\lambda}\boldsymbol{N}_1\boldsymbol{\lambda}\boldsymbol{W}\boldsymbol{R}_n - 2\left(\mathbf{Q}_m^C\right)^T\boldsymbol{N}_2\boldsymbol{\lambda}\boldsymbol{W}\boldsymbol{R}_n + \left(\mathbf{Q}_m^C\right)^T\boldsymbol{E}\mathbf{Q}_m^C \\ &\quad - 2\left(\tilde{\mathbf{Q}}_M\right)^T\boldsymbol{T}\boldsymbol{N}\boldsymbol{\lambda}\boldsymbol{W}\boldsymbol{R}_n + \left(\tilde{\mathbf{Q}}_M\right)^T\boldsymbol{\chi}\tilde{\mathbf{Q}}_M + 2\left(\mathbf{Q}_m^C\right)^T\boldsymbol{X}^T\left(\boldsymbol{T}\right)^T\tilde{\mathbf{Q}}_M\end{aligned} \tag{16}$$

where

$$\boldsymbol{N}_1=\int_0^1 \frac{\boldsymbol{B}_n^T\boldsymbol{B}_n}{\left(\boldsymbol{B}_n\boldsymbol{\lambda}\boldsymbol{\omega}\right)^2}ds, \boldsymbol{N}_2=\int_0^1 \frac{\left(\mathbf{B}_m^C\right)^T\boldsymbol{B}_n}{\boldsymbol{B}_n\boldsymbol{\lambda}\boldsymbol{\omega}}ds,$$

$$\boldsymbol{E}=\int_0^1 \left(\mathbf{B}_m^C\right)^T\mathbf{B}_m^C ds=\left(\frac{\binom{m}{i}\binom{m}{j}}{(2m+1)\binom{2m}{i+j}}\right)_{m\times m}, \ 0\le i,\ j\le m.$$

There are many numerical methods can be applied to solve λ [12], but for the stability, authority and repeatability of the method, we apply maple's functions *minimize*(*expr*, opt1, opt2, ..., optn) for the minimum value of $d_\lambda^2\left(\boldsymbol{r},\boldsymbol{q}\right)$, and *ApproximateInt*($f(x)$, $x=a..b$, opts) to realize numerical integration of the matrices $\boldsymbol{N}_1$ and $\boldsymbol{N}_1$, where arguments *method* = simpson and *partition* = 20, respectively.

5. Numerical examples

Several examples of approximation of rational Bézier curves by Bézier curves are presented in this section. For each example, we use Hausdoff distances to express error functions.

Example 1. The given curve is a rational Bézier curve of degree 2 with the control points $(0,0)$, $(1.2,1.5)$, $(1,0)$ and the associated weights 1, 3, 1. We produce 8, 9 and 10-degree Bézier curves satisfying $G^{(3,3)}$-continuity with the given curve respectively. Errors comparison of different degrees were given in Table 1. The graphs of distance functions $d_\lambda^2\left(\boldsymbol{r},\boldsymbol{q}\right)$ (16) for degrees illustrated in Figure 1(a) to show minimum value of λ . The resulting curves are illustrated in Figure 1 (b) and the corresponding error distance curves are shown in Figure 1 (c).

Example 2. The given curve is a rational Bézier of degree 4 with control points $(0,0)$, $(2,2)$, $(3,0)$, $(4,-2)$, $(4,0)$ and the associated weights $5,4,2,1,1$. We produce 3, 4 and 5-degree Bernstein-Jacobi hybrid curve satisfying $C^{(0,0)}$-continuity with the given curve. Table 2 is comparisons of

Table 1: Errors comparison of different degrees.

m	λ	Error
8	0.977520234167110	0.03705155951
9	0.977694721940438	0.03159070686
10	0.980670422354805	0.00448306784

approximation methods under Hausdorff distance. The graphs of distance function distance functions $d^2_\lambda(\boldsymbol{r}, \boldsymbol{q})$ (16) is illustrated in Figure 2(a) to show minimum value of λ. The resulting curves obtained by our method and Hu's method are shown in the Figure 2(b) and 2(d), respectively. The corresponding error distance curves are illustrated in the Figure 2(c) and 2(e), respectively.

Table 2: Error comparison of different degrees.

m	Our method		Hu's method	
	λ	Error	λ	Error
3	1.481286280	0.049976920855755	1.480160	0.06037148
4	1.279139695	0.016836651178081	1.305553	0.01689231
5	0.884817836	0.011527075552774	0.893806	0.01175240

Example 3. The given curve is a rational Bézier curve of degree 7 with control points $(0,0)$, $(0.5,2)$, $(1.5,2)$, $(2.5,-2)$,$(3.5,-2)$, $(4.5,2)$, $(5.5,2)$, $(6,0)$ and the associated weights $4, 10, 18, 8, 9, 40, 12, 20$. We produce a 5-degree Bézier curve satisfying $C^{(0,0)}$-continuity with the given curve. The parameter λ in our method is 0.704214485, while Hu's is 0.681401. The husdorff distance errors provided by our method and Hu's method are 0.06861713, and 0.074820, respectively. The graphs of distance functions $d^2_\lambda(\boldsymbol{r}, \boldsymbol{q})$ (16) for degrees illustrated in Figure 3(a) to show minimum value of λ . The resulting curves are illustrated in Figure 3 (b) and the corresponding error distance curves are shown in Figure 3(c).

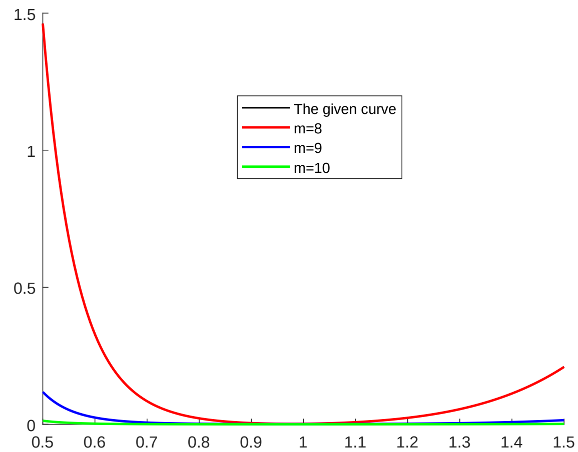

(a) The graphs of distance functions $d_\lambda^2\,(\boldsymbol{r},\boldsymbol{q})$ for degrees

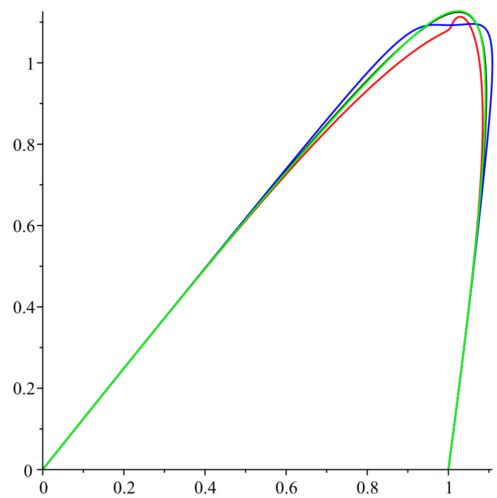

(b) The resulting curves

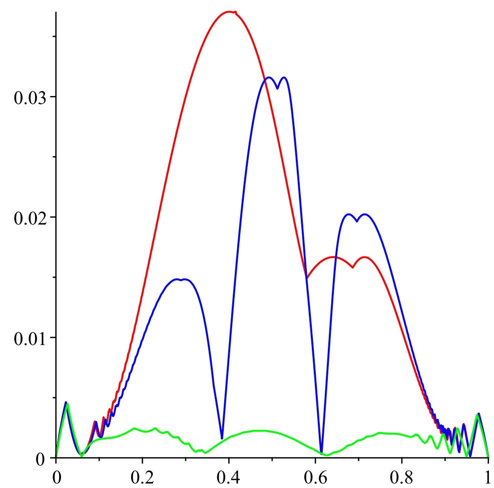

(c) The error distance curves

Figure 1: The graphs of distance functions, resulting curves and corresponding error distance curves

Example 4. The given curve is a rational Bézier curve of degree 9 with control points $(17,12)$, $(32,34)$, $(-23,24)$, $(33,62)$, $(-23,15)$, $(25,3)$, $(30,-2)$, $(-5,-8)$, $(-5,15)$, $(11,8)$ and the associated weights 1, 2, 3, 6, 4, 5, 3, 4, 2, 1. We produce a 10-degree Bézier curve satisfying $G^{(0,0)}$-continuity

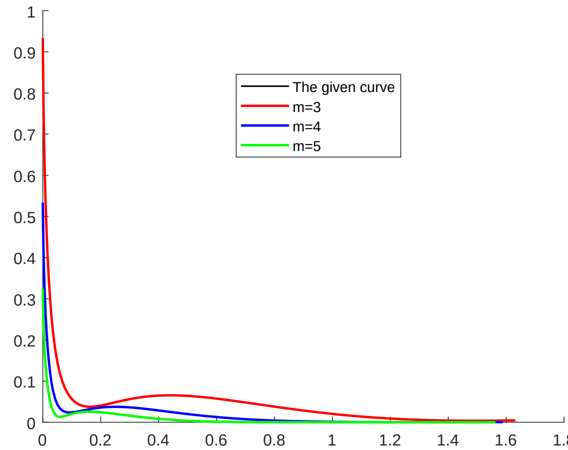

(a) The graphs of distance function $d_{\lambda}^{2}(\boldsymbol{r}, \boldsymbol{q})$ by our method

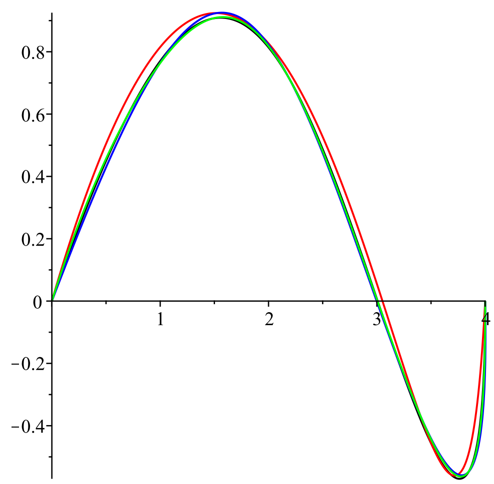

(b) The resulting curves obtained by our method

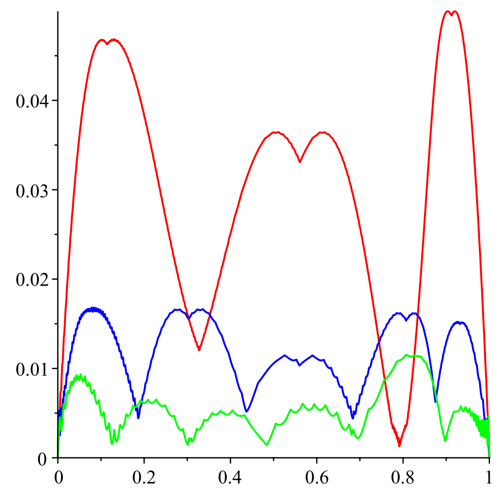

(c) The error distance curves by our method

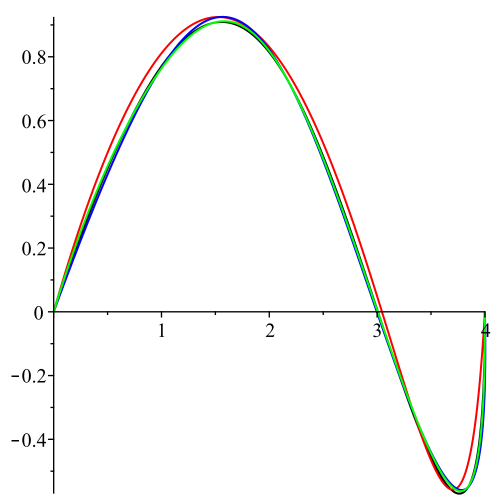

(d) The resulting curves obtained by Hu's method

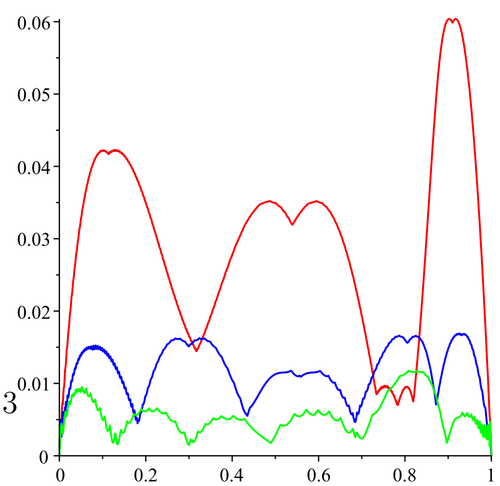

(e) The error distance curves by Hu's method

Figure 2: The graphs of distance functions, resulting curves and corresponding error distance curves

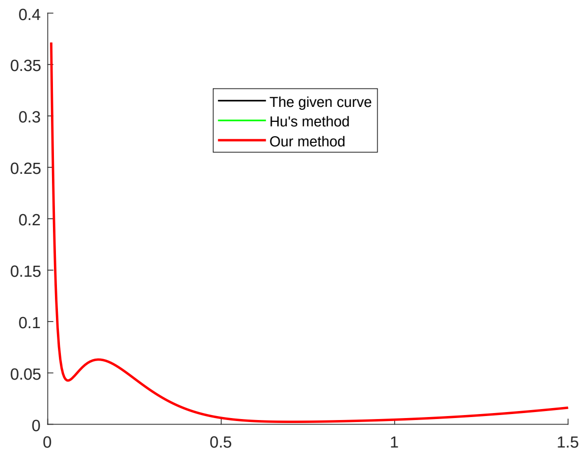

(a) The graph of distance function $d_\lambda^2\left(\boldsymbol{r}, \boldsymbol{q}\right)$ by our method

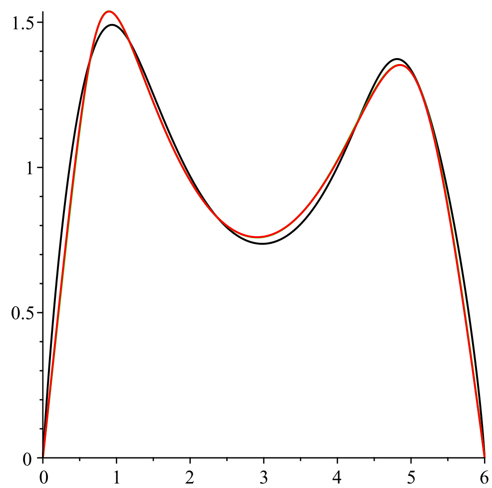

(b) The resulting curves

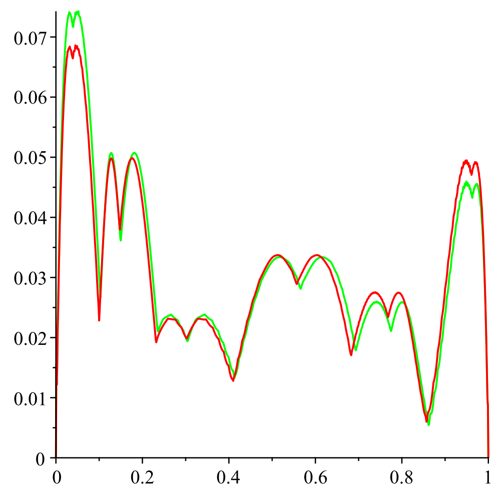

(c) The error distance curves

Figure 3: The graphs of distance functions, resulting curves and corresponding error distance curves

with the given curve. The parameter λ in our method is 0.86861029. The husdorff distance error provided by our method is 0.275802791948593. For the case $G^{(1,1)}$-continuity, the parameter λ is 0.875867536754241 and corresponding Hausdorff distance is 0.410850837381587. The graphs of distance

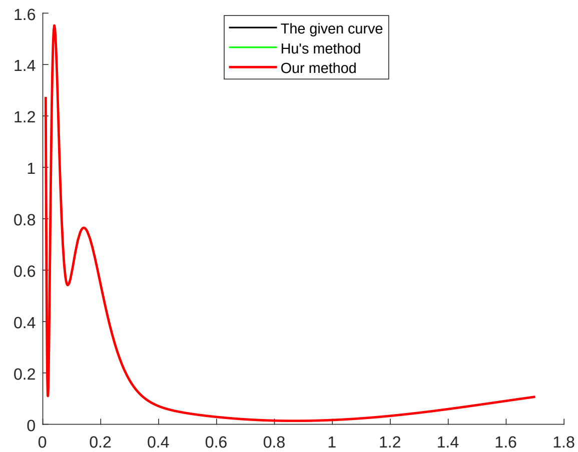

(a) The graph of distance function $d^2_\lambda(\boldsymbol{r},\boldsymbol{q})$ for $G^{(0,0)}$-continuity by our method

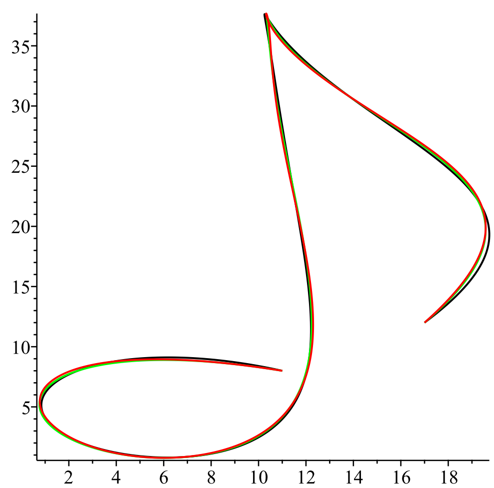

(b) The resulting curves

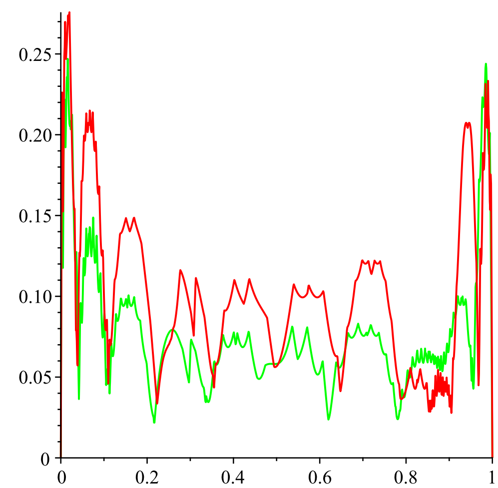

(c) The error distance curves

Figure 4: The graphs of distance functions, resulting curves and corresponding error distance curves with $G^{(0,0)}$-continuity

functions $d^2_\lambda(\boldsymbol{r},\boldsymbol{q})$ (16) for $G^{(0,0)}$ and $G^{(1,1)}$ -continuity illustrated in Figure 4(a) and 5(a) to show minimum value of λ, respectively . The resulting curves are illustrated in Figure 4 (b) and 5(b). The corresponding error distance curves are shown in Figure 4(c) and 5(c).

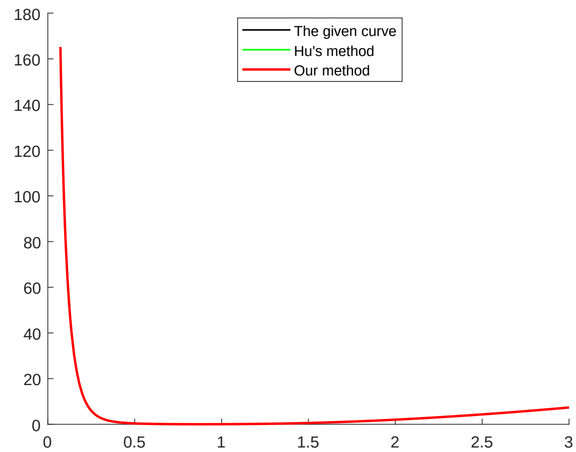

(a) The graph of distance function $d_\lambda^2(\boldsymbol{r}, \boldsymbol{q})$ for $G^{(1,1)}$-continuity by our method

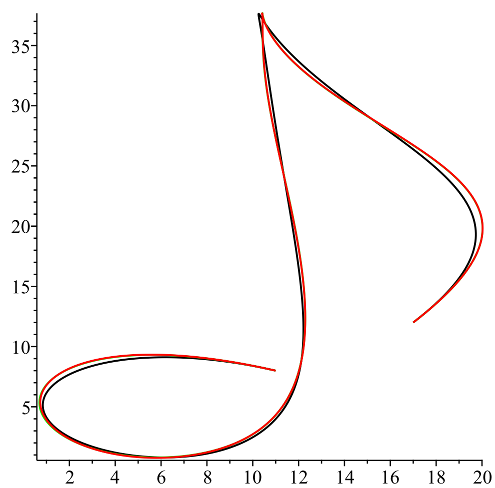

(b) The resulting curves

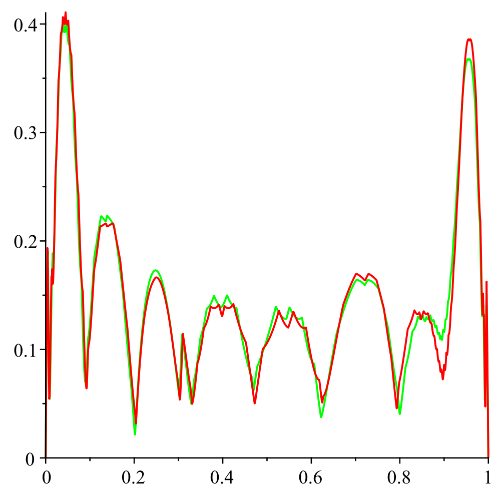

(c) The error distance curves

Figure 5: The graphs of distance functions, resulting curves and corresponding error distance curves with $G^{(1,1)}$-continuity

Conclusions

In this paper, we have proposed a reparameterization-based method for Jacobi-Bernstein hybrid polynomials approximating rational Bézier curves with constraints. The approximation curve and the given curve can satisfy parametric continuity or geometric continuity of any $u, v(u, v \geq 0)$ orders at two endpoints, respectively. Numerical examples show that our method has a better approximation effect than the previous methods under the Hausdorff distance. As for future work, the method can also be applied to the cases of rational tensor-product Bézier surfaces and rational triangular Bézier surfaces.

Acknowledgements

The work is supported by the Fundamental Research Funds for the Central Universities (GK201703007)

References

[1] Sederberg TW , Kakimoto M , Approximating rational curves using polynomial curves, in: G. Farin (Ed.), NURBS for Curve and Surface Design, SIAM, Philadelphia, 1991, pp. 149-158.

[2] Wang GJ , Sederberg TW, F.L. Chen, On the convergence of polynomial approximation of rational functions, Journal of Approximation Theory 89 (1997) 267-288.

[3] Wang GZ, Zheng JM, Bounds on the moving control points of hybrid curves, CVGIP: Graphical Models and Image Processing 59 (1) (1997) 19-25.

[4] Chen J, Wang GJ, Hybrid polynomial approximation to higher derivatives of rational curves, Journal of Computational and Applied Mathematics 235 (17) (2011) 4925-4936.

[5] Wang GJ, Tai CL, On the convergence of hybrid polynomial approximation to higher derivatives of rational curves, Journal of Computational and Applied Mathematics 214 (2008) 163-174.

[6] Cai HJ, Wang GJ , Constrained approximation of rational Bézier curves based on a matrix expression of its end points continuity condition, Computer-Aided Design 42 (2010) 495-504.

[7] Lewanowicz S, Woźny P ,Keller P, Polynomial approximation of rational Bézier curves with constraints, Numerical Algorithms 59 (4) (2012) 607-622.

[8] Shi M , Deng JS, Polynomial approximation of rational Bézier curves, Journal of Computational Information Systems 11 (20) (2015) 7339-7346.

[9] Xu G ,Kwok T ,Wang C C, et al. Isogeometric Computation Reuse Method for Complex Objects with Topology-Consistent Volumetric Parameterization[J]. Computer-aided Design, 2017: 1-13.

[10] Sederberg T W. Improperly parametrized rational curves[J]. Computer Aided Geometric Design, 1986, 3(1): 67-75.

[11] Cheng M ,Wu XJ,Pan YJ, Approximating rational Bézier curve with polunomial curve using re-parameterization, 2009 International Form on Computer Science-Technology and Applications,376-379.

[12] Hu Q Q,Xu HX, Constrained polynomial approximation of rational Bézier curves using reparameterization, Journal of Computational and Applied Mathematics 249 (2013) 133-143.

[13] Ahn Y, Degree reduction of Bézier curves with C^k-continuity using Jacobi polynomials. Computer Aided Geometric Design 2003;20:423-34.

[14] Chen G, Wang G , Optimal multi-degree reduction of Bézier curves with constraints of endpoints continuity, Computer Aided Geometric Design 19 (2002) 365-377.

[15] Farin G , Curves and Surfaces for Computer Aided Geometric Design, Academic Press, San Diego (1988).

[16] Farouki R T ,Rajan VT, Algorithms for polynomials in Bernstein form, Computer Aided Geometric Design 5 1-26(1988).

[17] Royden HL , Real Analysis. Prentice Hall (1988).

[18] Shi M , Wang GZ ,Kang BS, A geometric property of rational quadratic Bézier and its application, Journal of Northwest University (Natural Science Edition) 35(4) (2005) 377-378.

[19] Shi M , A note on the convergence of NURBS curves when weights approach infinity, 5th International Conference on Information Science and Control Engineering (2018) 73-74.